CLOUDSAT OBSERVES A LABRADOR SEA POLAR LOW

BY JOHN M. FORSYTHE AND JOHN M. HAYNES

The Arctic oceans give birth to intense mesoscale low-pressure systems, usually generated by outbreaks of cold, dry polar air over warm water. These systems are called polar lows. The classical polar low is included as a subtype that is restricted to maritime systems with near-surface winds exceeding 15 m s^{-1}. These types of polar lows can exhibit deep convection, a warm core, and lifetimes of a few hours to a few days. Sensible heat fluxes from the oceans play an important role in creating these systems, while latent heat fluxes can become important in their mature and decaying stage. They may appear visually similar to tropical cyclones on satellite imagery with an eyelike feature. Numerical simulations of polar lows are often unsuccessful. This can be due to poor initial and boundary conditions, model resolution, and the choice of cloud microphysical scheme. Due to their rapid genesis, small size, and occurrence over data-sparse oceans, polar lows pose a serious threat to mariners and coastal interests. Polar-orbiting satellite imagery could be culled to develop a useful database of polar lows, improving what we know about them and how they can be simulated.

Unlike tropical cyclones, polar lows are not routinely identified and tracked in real time. Their occurrence in high latitudes at the limits of usable geostationary satellite imagery makes tracking difficult. To obtain cases for scientific studies, including the improvement of polar low representation in numerical weather prediction models, these systems must be manually identified and matched with coincident data. The Norwegian Sea Surface Temperature and Altimeter Synergy (STARS) project (http://polarlow

FIG. 1. NASA Aqua MODIS instrument true-color visible image in the Labrador Sea, taken 1615 UTC 30 Nov 2013. *CloudSat* ground track across the polar low indicated by dashed red line.

.met.no/) has begun to detect and catalogue conditions that are favorable for polar low occurrence. The report of the 12th workshop of the European Polar Low Working Group in the September 2013 issue of *BAMS* provides an update on the latest polar low science.

Satellites are the primary tools used to observe polar lows, but a few aircraft studies have also been performed. The first aircraft lidar observations of a polar low were taken in 2008 over the Norwegian Sea, with highest cloud tops at 7 km. Since 2006, the NASA *CloudSat* satellite with a 94-GHz cloud radar and its companion lidar-carrying satellite *CALIPSO* have provided a new view of global clouds. *CloudSat* provides a nadir-only view of clouds with 240-m vertical resolution and 1.3-by-1.7-km horizontal resolution. A variety of science products—such as radar reflectivity and derived products including cloud liquid and ice water content, cloud bases and tops, and cloud classification—are available at www.cloudsat.cira.colostate.edu/. To aid in polar low identification,

AFFILIATIONS: FORSYTHE AND HAYNES—Cooperative Institute for Research in the Atmosphere, Colorado State University, Fort Collins, Colorado
CORRESPONDING AUTHOR: John M. Forsythe, Cooperative Institute for Research in the Atmosphere, 1375 Campus Delivery, Colorado State University, Fort Collins, CO 80523-1375
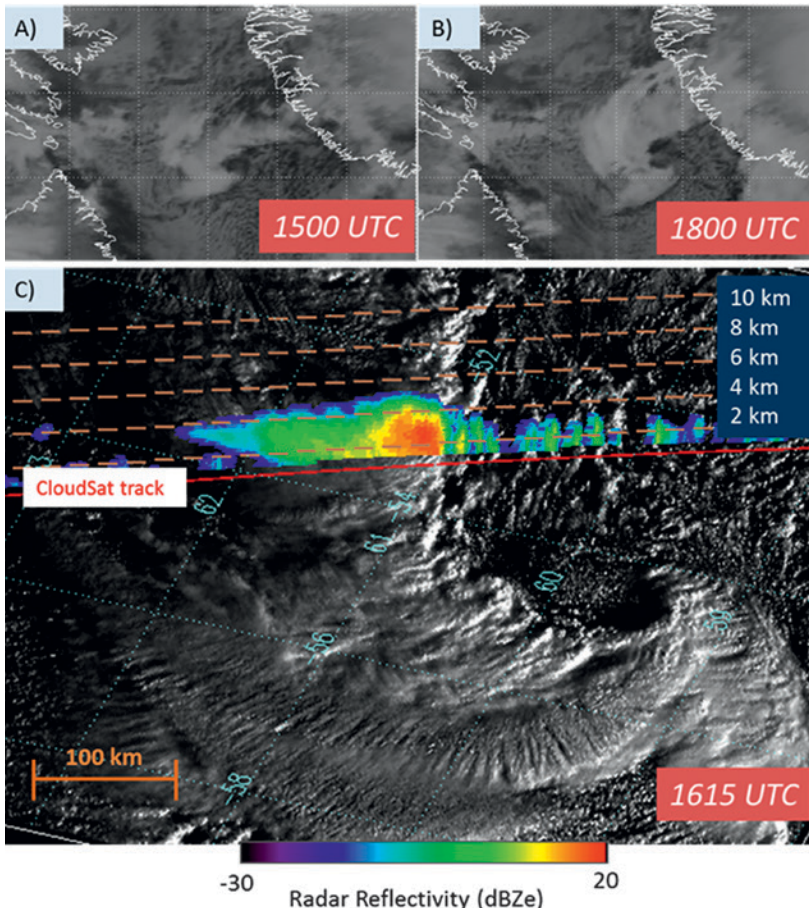E-mail: john.forsythe@colostate.edu

Fig. 2. Rapid evolution of the polar low at (a) 1500 UTC 30 Nov 2013 and (b) 1800 UTC in GOES-East infrared imagery. (c) *CloudSat* radar reflectivity profile superimposed on MODIS visible image at 1615 UTC 30 Nov 2013. The *CloudSat* track is indicated by the red line. Dashed brown lines are spaced 2 km vertically above sea level.

ing the classical appearance in satellite imagery. Temperatures at 500 hPa were between –40° and –45°C, favorable for polar low formation.

The evolution of the polar low and *CloudSat* radar cross-section is shown in Fig. 2. Two Geostationary Operational Environmental Satellite (GOES) infrared 11-µm images at 1500 and 1800 UTC bounding the *CloudSat* overpass indicate the rapid development of the polar low cloud shield. In Fig. 2c, the radar reflectivity cross section is overlaid on the MODIS visible image of the polar low. Reflectivity below 800 m is not plotted due to clutter from the surface. The highest reflectivity is in the 50 km-wide cloud band bordering the broken cloud to the south, with values of 20 dBZ. Radar-indicated cloud tops are 5 km, or at a pressure of about 500 hPa. The *CALIPSO* lidar also indicated highest cloud tops of approximately 5 km, indicating deep opaque clouds. Sloping returns from upper-level cloud streaming from the main polar low band occur north of 62°N.

It is likely that there are many more intersections of *CloudSat* and polar lows in the Arctic. Assuming a polar low diameter of 200 km at 60°N, a 24-h lifetime, and 40 polar lows per year in the Northern Hemisphere, about 5 polar lows per year should have coincident *CloudSat/CALIPSO* daytime overpasses. Since *CloudSat* data begins in 2006, this implies that about 40 daytime cases should be available to date. These cases would also be observed by the other sensors in the A-Train satellite formation with *CloudSat*. Collecting these cases into a *CloudSat* overpass database would be a useful endeavor. Such a database exists for tropical cyclones at the *CloudSat* website, and more than 350 *CloudSat* overpasses within 50 km of the tropical cyclone center have been identified to date. Such an effort applied to polar lows would help improve our understanding and modeling of these systems.

Cooperative Institute for Research in the Atmosphere (CIRA) resources were utilized to create a GOES-East infrared sector over the Labrador Sea with a 12-image loop updated at 3-h intervals. Criteria for manual identification and further examination of *CloudSat* products were first a classically appearing polar low during daylight, and then inspection of the *CloudSat* Quicklook imagery for an overpass in the vicinity.

A promising polar low case was identified in the Labrador Sea on 30 November 2013. The MODIS true color image of the polar low at 1615 UTC is shown in Fig. 1, with the *CloudSat* ground track indicated. The polar low had deep convection in a 50 km-wide band, an eyelike clear region, and radiating bands of upper-level cirrus. The NOAA RapidRefresh model analysis at 1600 UTC indicated 10-m wind speeds of 35–40 kt on the west side of the polar low, confirm-

FOR FURTHER READING

Heinemann, G., and Ø. Saetra, 2013: Workshop on polar lows. *Bull. Amer. Meteor. Soc.,* **94,** ES123–ES126, doi:10.1175/BAMS-D-12-00190.1.

Kolstad, E. W., 2011: A global climatology of favourable conditions for polar lows. *Quart. J. Roy. Meteor. Soc.,* **137,** 1749–1761, doi:10.1002/qj.888.

Parker, N., 1997: *Cold Air Vortices and Polar Low Handbook for Canadian Meteorologists.* 2d ed. Environment Canada, 102 pp.

Posselt, D. J., G. L. Stephens, and M. Miller, 2008: CLOUDSAT: Adding a new dimension to a classical view of extratropical cyclones. *Bull. Amer. Meteor. Soc.,* **89,** 599–609, doi:10.1175/BAMS-89-5-599.

Rasmussen, E. A., and J. Turner, 2003: *Polar Lows: Mesoscale Weather Systems in the Polar Regions.* Cambridge University Press, 612 pp.

Tourville, N., G. Stephens, M. DeMaria, and D. Vane, 2014: Remote sensing of tropical cyclones: Observations from *CloudSat* and A-Train profilers. *Bull. Amer. Meteor. Soc.,* **96**, 609–622, doi:10.1175/BAMS-D-13-00282.1.

Wagner, J. S., A. Gohm, A. Dörnbrack, and A. Schäfler, 2011: The mesoscale structure of a polar low: Airborne lidar measurements and simulations. *Quart. J. Roy. Meteor. Soc.,* **137,** 1516–1531, doi:10.1002/qj.857.

Zahn, M., and H. von Storch, 2008: A long-term climatology of North Atlantic polar lows. *J. Geophys. Res.,* **35,** L22702.